

Logistic Map Potentials

Thomas Curtright[§] and Andrzej Veitia[‡]

Department of Physics, University of Miami, Coral Gables, FL 33124-8046, USA

Abstract

We develop and illustrate methods to compute all single particle potentials that underlie the logistic map, $x \mapsto sx(1-x)$ for $0 < s \leq 4$. We show that the switchback potentials can be obtained from the primary potential through functional transformations. We are thereby able to produce the various branches of the corresponding analytic potential functions, which have an infinite number of branch points for generic $s > 2$. We illustrate the methods numerically for the cases $s = 5/2$ and $s = 10/3$.

I. INTRODUCTION

In two previous papers [1] it was shown how functions defined on a discrete lattice of time points may be smoothly interpolated in t , for a continuum of time points, through the use of solutions to Schröder's nonlinear functional equation [2]. If the effect of the first discrete time step is given as the map

$$x \mapsto f_1(x, s) , \quad (1)$$

for some parameter s , then Schröder's functional equation is

$$s\Psi(x, s) = \Psi(f_1(x, s), s) , \quad (2)$$

with Ψ to be determined. So, $f_1(x, s) = \Psi^{-1}(s\Psi(x, s), s)$. A continuous interpolation between the integer lattice of time points is then, for *any* t ,

$$f_t(x, s) = \Psi^{-1}(s^t\Psi(x, s), s) . \quad (3)$$

This can be a well-behaved, analytic and single-valued function of both x and t provided that $\Psi^{-1}(x, s)$ is a well-behaved, analytic, single-valued function of x , even though $\Psi(x, s)$ might be, and typically is, multi-valued. In this sense, analyticity in x leads to analyticity in t .

As discussed in [1], the interpolation can be envisioned as the trajectory of a particle passing through the initial x ,

$$x(t) = f_t(x, s) , \quad (4)$$

where the particle is moving according to Hamiltonian dynamics under the influence of a potential, V . Up to additive and multiplicative constants, at various times during the evolution of the particle, we have

$$V(x(t)) = - \left(\frac{dx(t)}{dt} \right)^2 . \quad (5)$$

At $t = 0$ this becomes $V(x) = - (\ln^2 s) \left(\frac{\Psi(x, s)}{d\Psi(x, s)/dx} \right)^2$. Thus, V may inherit multi-valuedness from Ψ [1].

At other times the x dependence of the potential also follows from that of the velocity profile of the interpolation, $dx(t)/dt$, when the latter is expressed as a function of $x(t)$. In general, this will exhibit the branches of the underlying analytic potential function. But more importantly for our purposes here, the various branches of the potential can also be determined directly from the functional equation V inherits from Ψ . This functional equation is

$$V(f_1(x, s), s) = \left(\frac{d}{dx} f_1(x, s) \right)^2 V(x, s) . \quad (6)$$

If the map (1) possesses a fixed point, we may attempt to solve this functional equation for V by series in x about that fixed point. We shall discuss in some detail the circumstances for which this series method is successful in the context of the logistic map $x \mapsto sx(1-x)$. In general, if the series can be constructed, it will of course have a finite radius of convergence. However, the series result can then be continued to other x by making use of the functional equation itself (a technique very familiar, e.g., for the Γ and ζ functions) and also by exploiting other special features for specific maps (cf. $s \rightarrow 2-s$ duality for the logistic map, discussed in Appendix A). These additional techniques will allow us to construct convergent series approximations for all branches of the potential in those situations where V is multi-valued. The net result is a family of potential sequences that encode for the corresponding continuous particle trajectories the various fixed points, bifurcations, limit cycles, and chaotic behavior of the discrete logistic map, for all s of interest.

[§]curtright@miami.edu [‡]aveitia@physics.miami.edu

II. FUNCTIONAL METHODS AND SERIES SOLUTIONS

Consider in detail the logistic map [3–7] on the unit interval, $x \in [0, 1]$,

$$x \mapsto sx(1-x) . \quad (7)$$

For the most part, we restrict our considerations to parameter values $s \in [0, 4]$. The maximum of the map is $s/4$, obtained from $x = 1/2$, so without loss of any essential features, we will also most often restrict $x \in [0, s/4]$. The map has fixed points at $x = 0$ and at $x_* = 1 - 1/s$. Schröder's equation for this map is

$$s\Psi(x, s) = \Psi(sx(1-x), s) , \quad (8)$$

and from this follows the functional equation for the underlying potential,

$$V(sx(1-x), s) = s^2(1-2x)^2 V(x, s) . \quad (9)$$

Applying the method of series solution about $x = 0$, with initial conditions that correspond to those used in [1] for the function $\Psi = x + \frac{1}{s-1}x^2 + \dots$, namely, $V(0, s) = 0$, $V'(0, s) = 0$, and $V''(0, s) = -2\ln^2 s$, we find:

$$V(x, s) = -(\ln^2 s) U(x, s) , \quad (10)$$

$$U(x, s) = x^2 \left(1 + \sum_{n=1}^{\infty} a_n(s) x^n \right) , \quad a_1 = \frac{2}{1-s} , \quad a_2 = \frac{5-3s}{(s-1)^2(s+1)} , \quad \dots . \quad (11)$$

The higher coefficients in the expansion are determined recursively by

$$a_{n+2} = \frac{1}{(1-s^{n+2})} \left(4a_{n+1} - 4a_n + \sum_{j=1+\lfloor \frac{n-1}{2} \rfloor}^{n+1} (-1)^{n-j} a_j s^j \binom{j+2}{n+2-j} \right) \quad \text{for } n \geq 1, \quad (12)$$

where $\lfloor \dots \rfloor$ is the floor function. In principle, this series solves (9) for any s , within its radius of convergence.

Based on numerical studies, we infer the radius of convergence [8] of the series depends on s as follows:

$$R(s) = \frac{1}{\limsup_{n \rightarrow \infty} (|a_n(s)|^{1/n})} = \begin{cases} \frac{1}{2} & \text{if } 0 < s \leq \frac{2}{3} , \\ \left| 1 - \frac{1}{s} \right| & \text{if } \frac{2}{3} \leq s \leq 2 , \\ \frac{s}{4} & \text{if } 2 \leq s \leq 4 . \end{cases} \quad (13)$$

For $0 < s \leq 2/3$, and also for $2 \leq s \leq 4$, the $|a_n|$ are monotonic for large n and the radius immediately follows either from the limsup expression in (13) or from the simple ratio test, $R(s) = \lim_{n \rightarrow \infty} |a_{n-1}(s)/a_n(s)|$. But for $2/3 < s < 2$, there is spiky behavior in $|a_{n-1}/a_n|$ for intervals in n , which makes it difficult to use the simple ratio test to determine R . This is because the $|a_n(s)|$ are not monotonic functions of n for these values of s . Occasionally the coefficients become small before changing sign. Fortunately, the limsup expression for R circumvents this spiky behavior to yield the values given in (13) for all s .

It is not difficult to work out explicit series results for $U(x, s)$, for generic s , say to $O(x^{12})$. Such polynomials in x are sufficient approximations to obtain the graphics to follow, when augmented with functional methods to be described. Based on those explicit results, we infer that the series involve numerator polynomials, $p_n(s)$, of order $1 + (n-2)(n-1)/2$ in s , as well as “s-factorials” in the following form:

$$(s-1)^2 U(x, s) = x^2 \left((s-1)^2 - 2(s-1)x + \sum_{n=2}^{\infty} \frac{p_n(s)}{[n]_s!} x^n \right) . \quad (14)$$

Here, deformed integers and factorials are defined by: $[k]_s = \frac{s^k - 1}{s - 1}$, and $[n]_s! = \prod_{k=1}^n [k]_s$. The recursion relation for the polynomials follows from that for $a_n(s)$. It involves a mix of ordinary and deformed integers:

$$p_{n+2}(s) = \frac{1}{1-s} \left(4p_{n+1}(s) - 4[n+1]_s p_n(s) + [n+1]_s! \sum_{j=1+\lfloor \frac{n-1}{2} \rfloor}^{n+1} \frac{(-1)^{n-j}}{[j]_s!} \binom{j+2}{n+2-j} s^j p_j(s) \right) . \quad (15)$$

This recursion relation is seeded by

$$p_1(s) = 2(1-s) \ , \quad p_2(s) = 5 - 3s \ . \quad (16)$$

As written, it looks rather miraculous that the $\frac{1}{1-s}$ prefactor in (15) is always canceled. Nevertheless, it is. This follows from $\lim_{s \rightarrow 1} p_n(s)$, but we have not yet determined an elegant proof of this fact.

As originally obtained by Schröder, there are three closed-form solutions known for Ψ , for $s = -2, 2$, and 4 . These are:

$$\begin{aligned} \Psi(x, -2) &= \frac{\sqrt{3}}{6} \left(2\pi - 3 \arccos \left(x - \frac{1}{2} \right) \right) \ , \quad \Psi^{-1}(x, -2) = \frac{1}{2} - \cos \left(\frac{2x}{\sqrt{3}} + \frac{\pi}{3} \right) \ , \\ \Psi(x, 2) &= -\frac{1}{2} \ln(1-2x) \ , \quad \Psi^{-1}(x, 2) = \frac{1}{2} (1 - e^{-2x}) \ , \\ \Psi(x, 4) &= (\arcsin \sqrt{x})^2 \ , \quad \Psi^{-1}(x, 4) = (\sin \sqrt{x})^2 \ . \end{aligned} \quad (17)$$

Note that while the Ψ are multi-valued the inverse functions are all single-valued. The corresponding closed-form expressions for

$$U(x, s) = \left(\frac{\Psi(x, s)}{d\Psi(x, s)/dx} \right)^2 \quad (18)$$

are also multi-valued and follow immediately:

$$U(x, s = -2) = \frac{1}{36} (1+2x)(3-2x) \left(2\pi - 3 \arccos \left(x - \frac{1}{2} \right) \right)^2 \ , \quad (19)$$

$$U(x, s = 2) = \frac{1}{4} (1-2x)^2 \ln^2(1-2x) \ , \quad (20)$$

$$U(x, s = 4) = x(1-x) \arcsin^2 \sqrt{x} \ . \quad (21)$$

Were we to start from these expressions for U , we could recover Ψ by solving and integrating (18). Another way to express the result for $s = 4$ is similar in form to that for $s = -2$, namely,

$$U(x, s = 4) = \frac{1}{4} x(1-x) (\pi - \arccos(2x-1))^2 \ . \quad (22)$$

Indeed, it is well-known that the logistic maps for $s = 4$ and $s = -2$ are intimately related through the functional conjugacy of the underlying Schröder equations. (See Appendix A.)

III. OBTAINING THE SWITCHBACK POTENTIALS

The sequence of switchback potentials, i.e. the various branches of the analytic potential function, can be obtained from the functional equation for the potential. (The same procedure also works to give the branch structure of the Schröder Ψ function. For an example, see Appendix B.) This follows from (8) and (18), namely,

$$U(sx(1-x)) = s^2(1-2x)^2 U(x) \ . \quad (23)$$

Next we write $y = sx(1-x)$, so then $x_{\pm} = \frac{1}{2} \left(1 \pm \sqrt{1-4y/s} \right)$ and $(1-2x_{\pm})^2 = 1-4y/s$. Thus the previous relation is just $U(y) = s(s-4y) U(x_{\pm})$. Now, we rename $y \rightarrow x$ to obtain

$$x_{\pm} = \frac{1}{2} \pm \frac{1}{2} \sqrt{1-4x/s} \ , \quad (24)$$

$$U_{\pm}(x) \equiv s(s-4x) U(x_{\pm}) = s(s-4x) U \left(\frac{1}{2} \pm \frac{1}{2} \sqrt{1-4x/s} \right) \ . \quad (25)$$

One of these potentials (U_-) reproduces the original series for the primary potential expanded about $x = 0$, as may be seen by direct comparison of the series or by numerical evaluation. Alternatively, the other (U_+) gives the potential on another sheet of the function's Riemann surface, hence the first switchback potential for $s > 2$. This is easily checked against the closed-form results for the $s = 4$ case.

Since U_- has built into it zeroes at both $x = 0$ and $x_{\max} = s/4$, it is actually a more useful form than just the series about $x = 0$. When $2 < s \leq 4$, the series has radius of convergence $R(s) = s/4$. However, from

using U_- instead of the direct series, we have convergence over the whole closed interval, $x \in [0, s/4]$, since then $0 \leq \frac{1}{2} - \frac{1}{2}\sqrt{1-4x/s} \leq 1/2 < R(s)$ when $2 < s \leq 4$. Thus we need only evaluate U appearing in U_- within the region of convergence of its series about zero. That is to say, first construct the series for U , and then from that series build U_- . Finally, identify this with U_0 , the primary potential in the sequence.

Similarly, U_+ may be identified with the first switchback in the sequence, U_1 , but for better convergence properties it is useful to build U_+ from U_0 instead of U . By doing this when $2 < s \leq 4$, we have convergence over the whole closed sub-interval, $x \in [\frac{1}{16}s^2(4-s), s/4]$, with zeroes of U_1 built-in at the end-points of the interval.

So the primary potential and the first switchback are well-represented by

$$U_0(x) = s(s-4x) U\left(\frac{1}{2} - \frac{1}{2}\sqrt{1-4x/s}\right), \quad (26)$$

$$U_1(x) = s(s-4x) U_0\left(\frac{1}{2} + \frac{1}{2}\sqrt{1-4x/s}\right). \quad (27)$$

In the first of these expressions, U is given by the direct series solution of the functional equation (23).

Now, go through this procedure all over again, beginning with $U(sy(1-y)) = s^2(1-2y)^2 U(y)$. Let $z = sy(1-y)$. Then $y_{\pm} = \frac{1}{2}\left(1 \pm \sqrt{1-4z/s}\right)$ and $U(z) = s(s-4z)U(y_{\pm}) = s(s-4z)s(s-4y_{\pm})U((x_{\pm})_{\pm})$ where $x_{\pm\pm} = \frac{1}{2}\left(1 \pm \sqrt{1-4y_{\pm}/s}\right)$ with any combination of \pm s allowed. Therefore $U(z) = s(s-4z)s\left(s-2\left(1 \pm \sqrt{1-4z/s}\right)\right) \times U\left(\frac{1}{2} \pm \frac{1}{2}\sqrt{1-\frac{2}{s}\left(1 \pm \sqrt{1-4z/s}\right)}\right)$. Again, rename $z \rightarrow x$ to obtain

$$U_{\pm\pm}(x) = s(s-4x)U_{\pm}(x_{\pm}) = s(s-4x)s\left(s-2\left(1 \pm \sqrt{1-4x/s}\right)\right) U\left(\frac{1}{2} \pm \frac{1}{2}\sqrt{1-\frac{2}{s}\left(1 \pm \sqrt{1-4x/s}\right)}\right), \quad (28)$$

with any combination of \pm s allowed. And to improve the convergence properties of this expression, replace U on the RHS with U_0 .

This process may be continued indefinitely, through successive application of the basic substitution $U(x) \rightarrow s(s-4x)U(x_{\pm})$. For example, the next set of potentials in the sequence is $U_{\pm\pm\pm}(x) = s(s-4x)U_{\pm\pm}(x_{\pm})$, etc. In general, the n th iteration of the procedure gives

$$\underbrace{U_{\pm\pm\pm\dots\pm}}_{n \text{ times}}(x) = s(s-4x)\underbrace{U_{\pm\pm\pm\dots\pm}}_{n-1 \text{ times}}(x_{\pm}). \quad (29)$$

Finally, at each iteration, we must select appropriate switchback potentials out of the 2^n different expressions. In particular, we note that many of the $U_{\pm\pm\dots\pm}(x)$ will be complex-valued for the x intervals under consideration, and therefore they are not of immediate interest since they do not govern the particle's evolution along the real axis. (The continuation of the particle trajectory into the complex plane is outside the scope of this paper.)

IV. NUMERICAL EXAMPLES

A. The potential sequence for $2 < s \leq 3$

These are values of the parameter for which the discrete logistic map converges to a single fixed point: There are no bifurcations. Nevertheless, there are two sign choices when the functional equation for the potential is applied once, four choices when it is applied twice, and so on.

$$V_{\pm}(x, s) = s(s-4x)V_0\left(\frac{1}{2} \pm \sqrt{\frac{1}{4} - \frac{x}{s}}, s\right) \quad (30)$$

$$V_{\pm\pm}(x, s) = s(s-4x)s\left(s-2\left(1 \pm \sqrt{1-4x/s}\right)\right)V_0\left(\frac{1}{2} \pm \sqrt{\frac{1}{4} - \frac{1}{s}\left(\frac{1}{2} \pm \sqrt{\frac{1}{4} - \frac{x}{s}}\right)}, s\right). \quad (31)$$

As it turns out from numerical studies, for $2 < s \leq 3$ only the positive sign choices are needed to produce the sequence of switchback potentials.

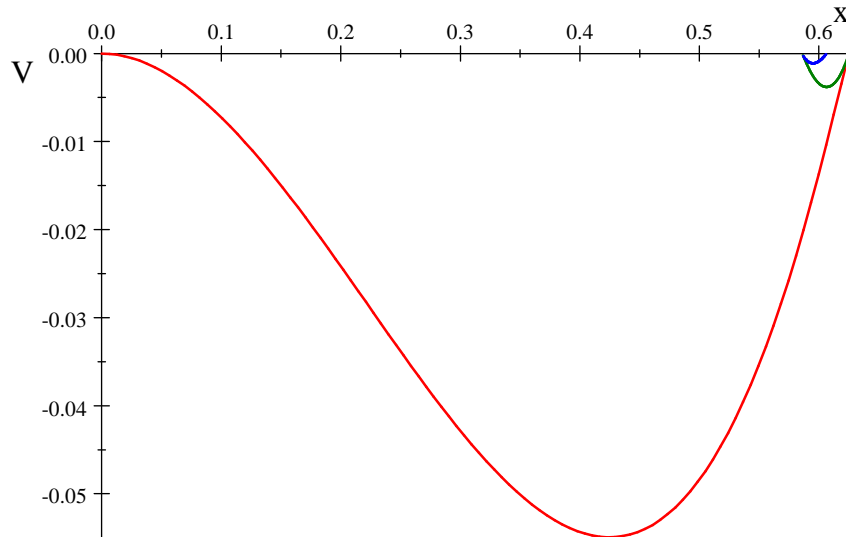
$$V_1(x, s) = s(s-4x)V_0\left(\frac{1}{2} + \sqrt{\frac{1}{4} - \frac{x}{s}}, s\right), \quad V_2(x, s) = s(s-4x)V_1\left(\frac{1}{2} + \sqrt{\frac{1}{4} - \frac{x}{s}}, s\right), \quad (32)$$

etc. In general, there is a recursion relation,

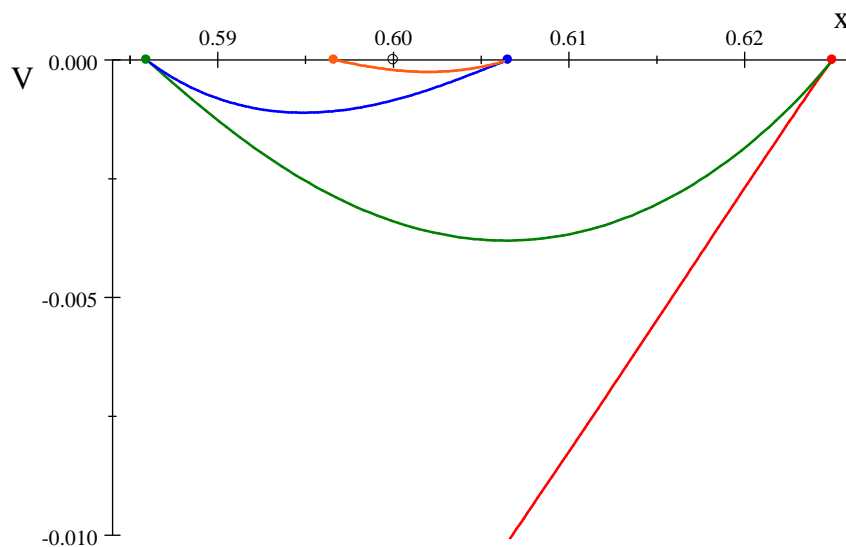
$$V_{n+1}(x, s) = s(s - 4x) V_n \left(\frac{1}{2} + \sqrt{\frac{1}{4} - \frac{x}{s}}, s \right). \quad (33)$$

The evolving particle moves through this sequence of potentials in succession, with the potential index incrementing up by one each time the particle encounters a turning point.

Consider the specific case $s = 5/2$. This is representative for $2 < s \leq 3$. For this case, the turning points converge onto the nontrivial fixed point $x_* = 1 - 1/s = 3/5$. This is evident in the following graphs.



V_0 in red, V_1 in green, and V_2 in blue, for $s = 5/2$. The first upper turning point is $x = 5/8$. Subsequent lower and upper turning points are obtained just by iterating the $s = 5/2$ logistic map, starting with $x = 5/8$, and are shown on the next magnified graph as colored points.



V_0 in red, V_1 in green, V_2 in blue, and V_3 in orange, for $s = 5/2$. The first upper turning point is $x = 5/8$, the first lower turning point is $x = \frac{75}{128} = 0.58594$, the second upper turning point is $x = \frac{19875}{32768} = 0.60654$, etc., as obtained by map iteration. The nontrivial fixed point is at $x_* = 3/5$, indicated by the black circle on the x axis.

As the zero-energy particle moves through this sequence of increasingly shallow, narrowing potentials, its average speed decreases, giving the *appearance* of a dissipative system. Nevertheless, even as the particle motion subsides upon convergence into the fixed point at $x = 3/5$, energy is rigorously conserved through changes in the potential.

Insofar as the turning points are branch points for the corresponding analytic potential function, and the various switchback potentials are just the values of that analytic function on the various sheets of its Riemann surface, this is convincing numerical evidence for that function to have an infinite number of such branch points, for generic s .

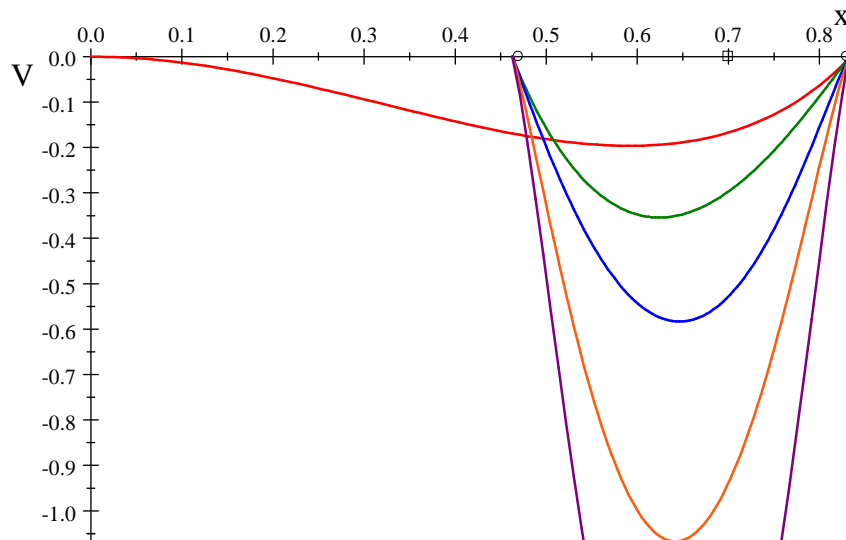
While of course there are many well-known functions with this property (for example, the inverses of Bessel functions, $J_n^{-1}(x)$), this would seem to account for the historical fact that closed-form solutions have *not* been found for generic s , or even for specific s , except in those very special cases where the number of branch points is one or two. Recall the exact closed-form cases $s = 2$ and $s = 4$ have analytic potential functions with one and two branch points, respectively, as evident in (20) and (21).

We may check numerically the transit times for each potential in the sequence: $\Delta t_n = 1$, for $n \geq 1$, within the expected uncertainties for truncation of the series (11). For example, using Mathematica to compute the initial series (11) to 200th order and also to evaluate the numerical integrations, we find $\int_{1/2}^{5/8} \frac{dx}{\sqrt{-V_0}} = 1.000000$, $\int_{75/128}^{5/8} \frac{dx}{\sqrt{-V_1}} = 1.000000$, $\int_{75/128}^{19875/32768} \frac{dx}{\sqrt{-V_2}} = 1.000000$, $\int_{1281241875/2147483648}^{19875/32768} \frac{dx}{\sqrt{-V_3}} = 1.000000$, etc., corresponding to the iterations $\frac{5}{2}x(1-x)|_{x=1/2} = \frac{5}{8}$, $\frac{5}{2}x(1-x)|_{x=5/8} = \frac{75}{128}$, $\frac{5}{2}x(1-x)|_{x=75/128} = \frac{19875}{32768}$, $\frac{5}{2}x(1-x)|_{x=19875/32768} = \frac{1281241875}{2147483648}$, etc. These transit times are consistent with the continuously evolving, zero-energy particle moving under the influence of each of the potentials in succession, $V_0 \rightarrow V_1 \rightarrow V_2 \rightarrow \dots$, thereby converging onto the fixed point at $x = 3/5$. The numbers confirm that for cases with $2 < s \leq 3$, only positive roots are needed to obtain all the switchback potentials, as previously indicated in (33).

B. The potential sequence family for $3 < s < 4$

These are values of the parameter for which the discrete logistic map produces bifurcations and asymptotes to limit cycles, rather than unique fixed points, and as s is increased, chaotic behavior erupts. Generally speaking, for these values of s the analytic potentials driving the trajectories are more complicated than for $s \leq 3$, and their branches are not so easy to enumerate as they are encountered by the evolving particle. The potentials here may be grouped into a *family of sequences*, where potentials with common upper and lower turning points constitute a single member of the family. From one family member to the next, for fixed sequence index, the potentials exhibit a progressive shallowing (similar to the behavior of the individual potentials for $s = 5/2$). However, the V s for a given family member successively deepen as the sequence index increases. Consequently, the locally averaged speed of the particle moving through the potentials does not necessarily diminish, but often increases, giving the *appearance* of a driven system. Nevertheless, energy is still rigorously conserved.

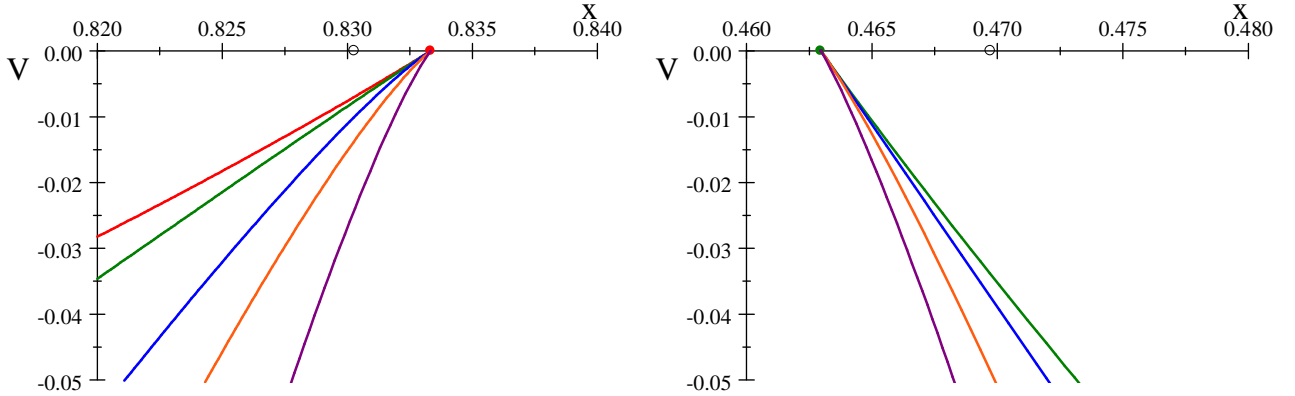
The limit cycle situation may be illustrated by the case $s = 10/3$, while the chaotic situation is aptly illustrated by the uppermost value, $s = 4$. The latter case was fully discussed in [1], and originally led to the notion of the switchback potentials. On the other hand, the potential structure for the $s = 10/3$ case is more complicated than for $s = 4$, the latter having only one member for its family of potential sequences, and in fact $s = 10/3$ is much more representative of the situation for generic parameter values in the range $3 < s < 4$. Therefore, we discuss $s = 10/3$ in some detail. This case evolves towards a two-cycle, consisting of the points $\frac{1}{20}\sqrt{13} + \frac{13}{20} = 0.830278$ and $\frac{13}{20} - \frac{1}{20}\sqrt{13} = 0.469722$. The first few terms in the potential sequence (33) are shown here, for this particular s .



V_0 in red, V_1 in green, V_2 in blue, V_3 in orange, and V_4 in purple, for $s = 10/3$. The upper turning point is $x = 5/6$. The two-cycle points are small black circles on the axis. The small black square is the nontrivial fixed point of the map, $x_* = 7/10$, and is revisited after integer time steps, but it is not a fixed point for the continuous evolution.

Deepening of the V s is evident for this “mother sequence.” The turning points for this sequence do *not* converge in this $s = 10/3$ case. Rather, they are fixed at $\frac{5}{6}$ for the upper turning point, and $\frac{25}{54}$ for the lower turning point, the

latter obtained by acting on the former with the $s = \frac{10}{3}$ discrete logistic map : $\frac{5}{6} = 0.833\ 333 \mapsto \frac{25}{54} = 0.462\ 963$. While these points are not far from the two-cycle points, as evident below, close does not count (except when playing pétanque).



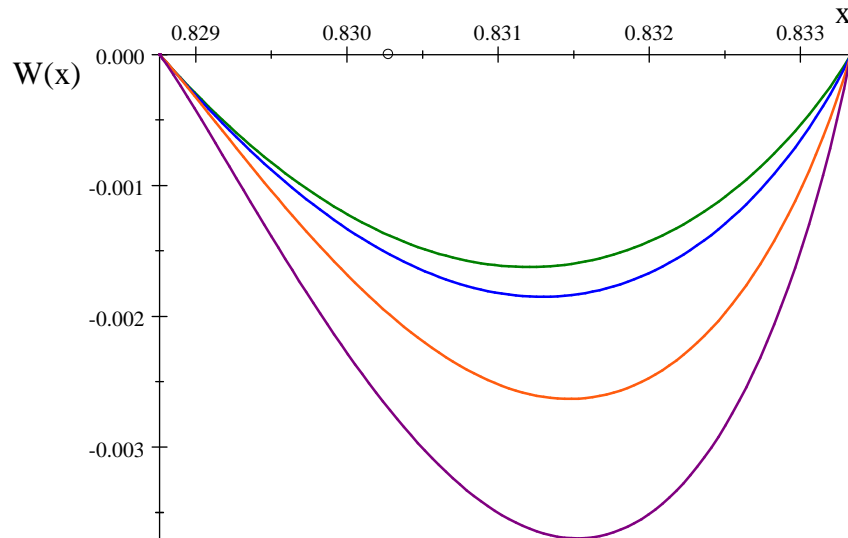
V_0 red, V_1 green, V_2 blue, V_3 orange, & V_4 purple, for $s = 10/3$.
 $s = 10/3$. The upper turning point is $x = \frac{5}{6}$. The lower turning point is $x = \frac{25}{54}$.

Other sequences in the family of potentials are needed to achieve convergence of the continuous particle trajectory, for unit time steps, onto the two-cycle of the map.

So, we define a second sequence in the family of potentials by changing the sign of the root in the arguments of the potentials in the first sequence, while noting that $W_0(x, s) = s(s - 4x) V_0\left(\frac{1}{2} - \sqrt{\frac{1}{4} - \frac{x}{s}}, s\right)$ just reproduces V_0 . More interesting cases of these “offspring” potentials are given by

$$W_n(x, s) = s(s - 4x) V_n\left(\frac{1}{2} - \sqrt{\frac{1}{4} - \frac{x}{s}}, s\right), \quad \text{for } n \geq 1. \quad (34)$$

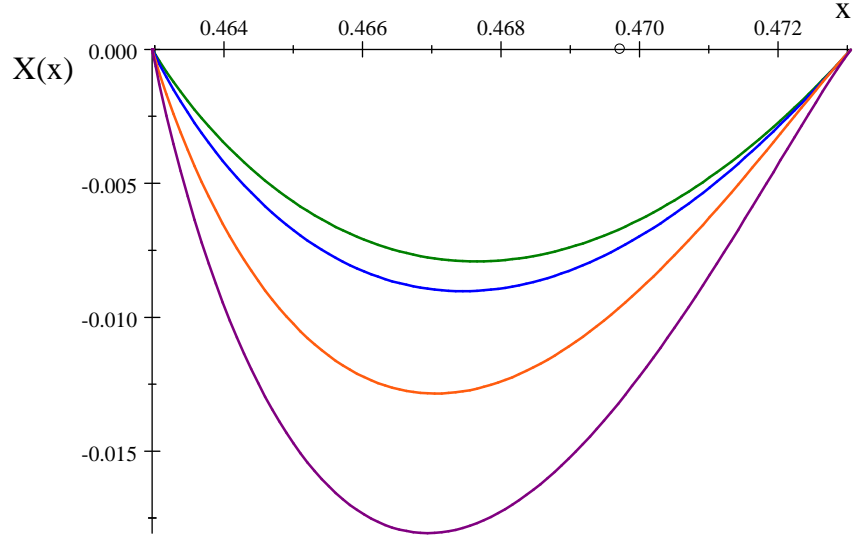
These do *not* reproduce any of the previous potentials. We plot a few for the $s = 10/3$ case.



W_1 green, W_2 blue, W_3 orange, and W_4 purple, for $s = 10/3$.

For this second sequence the lower turning point can be obtained by acting with the discrete map on the lower turning point for the first sequence, i.e. $\frac{25}{54} = 0.462\ 963 \mapsto \frac{3625}{4374} = 0.828\ 761$, while the upper turning point remains the same as for the first sequence, i.e. $\frac{5}{6} = 0.833\ 333$. Continuing the enumeration of the potential family members, we define a third sequence of potentials, and we plot a few.

$$X_n(x, s) = s(s - 4x) W_n\left(\frac{1}{2} + \sqrt{\frac{1}{4} - \frac{x}{s}}, s\right), \quad \text{for } n \geq 1, \quad (35)$$



X_1 green, X_2 blue, X_3 orange, and X_4 purple, for $s = 10/3$.

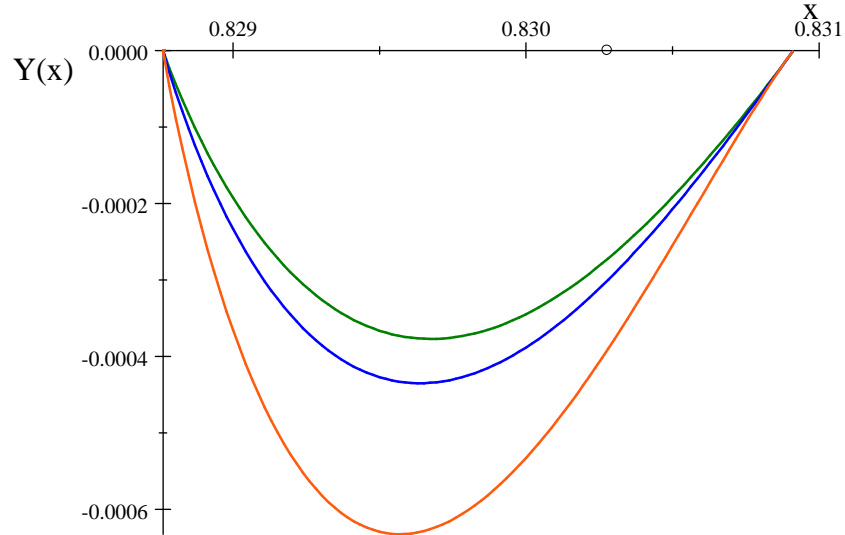
For this third sequence the lower turning point remains the same as for the first sequence, i.e. $\frac{25}{54} = 0.462963$, while the upper turning point can be obtained by acting with the discrete map on the lower turning point for the second sequence, i.e. $\frac{3625}{4374} = 0.828761 \mapsto \frac{13575625}{28697814} = 0.473054$.

This procedure may be continued indefinitely. We define fourth and fifth sequences as[†]

$$Y_n(x, s) = s(s - 4x) X_n \left(\frac{1}{2} - \sqrt{\frac{1}{4} - \frac{x}{s}}, s \right), \quad (36)$$

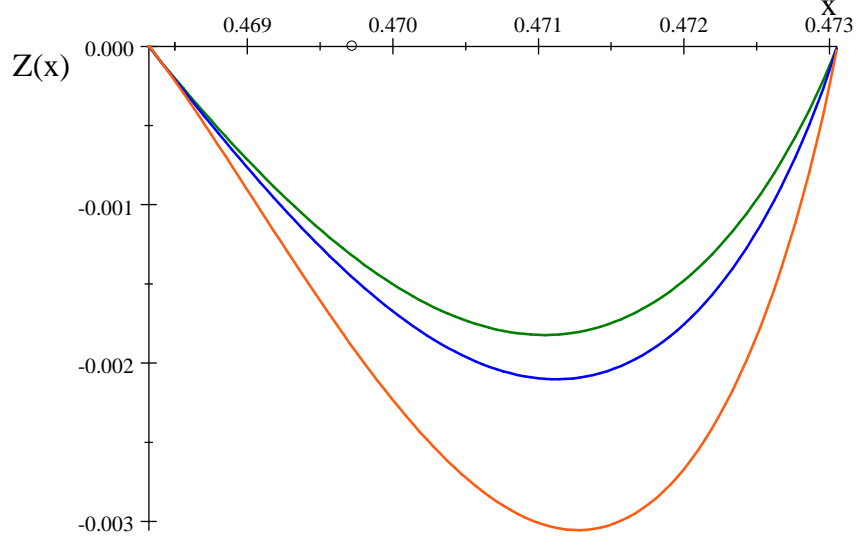
$$Z_n(x, s) = s(s - 4x) Y_n \left(\frac{1}{2} + \sqrt{\frac{1}{4} - \frac{x}{s}}, s \right), \quad (37)$$

etc., and we plot the first few of these new sequences.



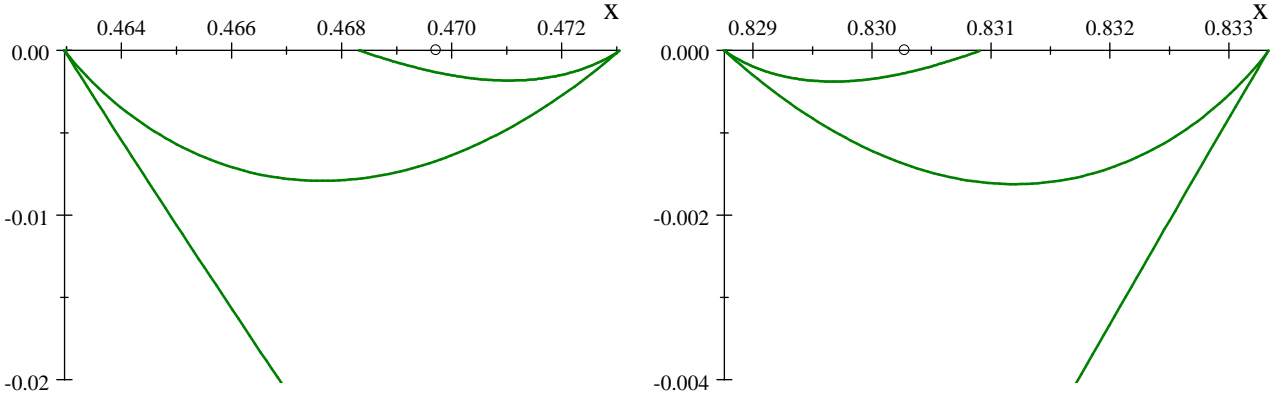
Y_1 green, Y_2 blue, and Y_3 orange, for $s = 10/3$.

[†]A more systematic notation would employ two potential indices, to denote an infinite matrix of potentials. For example, we could designate $V_n = V_n^{(0)}$, $W_n = V_n^{(1)}$, $X_n = V_n^{(2)}$, $Y_n = V_n^{(3)}$, $Z_n = V_n^{(4)}$, etc. The super-index here is the *family number*.



Z_1 green, Z_2 blue, and Z_3 orange, for $s = 10/3$.

The story here is somewhat analogous to, but more complicated than, the situation for $2 < s \leq 3$. Instead of individual potentials in the sequence $\{V_n\}$ converging onto the fixed point, as would be the case for $2 < s \leq 3$, here each of the individual V_n has proliferated into a “sideways” sequence of potentials, $\{V_n, W_n, X_n, Y_n, Z_n, \dots\}$, which converge to the points in the 2-cycle. To show what we mean by this, we plot $\{V_1, W_1, Y_1\}$ and $\{V_1, X_1, Z_1\}$ near the lower and upper points, respectively, in the two-cycle.



$V_1, W_1,$ and Y_1 near the lower point in the two-cycle for $s = 10/3$. $V_1, X_1,$ and Z_1 near the upper point in the two-cycle for $s = 10/3$.

This type of behavior is repeated by $\{V_n, W_n, Y_n\}$ and $\{V_n, X_n, Z_n\}$ for each n .

To complete the picture for the evolving particle, it is necessary to understand the order in which the potentials act, i.e. to determine how the switches are made from one potential to another as the turning points are encountered by the particle. Unlike the situation with $s \leq 3$, here this can be a bit tedious. From a numerical examination of various transit times (and also from the branch structure of the underlying Schröder auxiliary function, as exhibited in Appendix B) we infer the order of the potentials for the $s = 10/3$ case to produce a *chemin des énergies potentielles*:

$$V_0 \rightarrow \underbrace{V_1}_{\Delta t=1} \rightarrow \underbrace{V_2 \rightarrow W_1}_{\Delta t=1} \rightarrow \underbrace{W_2 \rightarrow V_3 \rightarrow X_1}_{\Delta t=1} \rightarrow \underbrace{X_2 \rightarrow V_4 \rightarrow W_3 \rightarrow Y_1}_{\Delta t=1} \rightarrow \underbrace{Y_2 \rightarrow W_4 \rightarrow V_5 \rightarrow X_3 \rightarrow Z_1}_{\Delta t=1} \rightarrow \dots, \quad (38)$$

etc. Here we have also indicated how the potentials combine into groups with unit total transit time. For example, again using Mathematica to compute the initial series (11) to 200th order and computing the transit times numerically, we find: $\int_{25/54}^{5/6} \frac{dx}{\sqrt{-V_1}} = 1.000000$; $\int_{25/54}^{5/6} \frac{dx}{\sqrt{-V_2}} + \int_{3625/4374}^{5/6} \frac{dx}{\sqrt{-W_1}} = 0.825728 + 0.174272 = 1.000000$; $\int_{25/54}^{5/6} \frac{dx}{\sqrt{-V_3}} + \int_{25/54}^{13575625/28697814} \frac{dx}{\sqrt{-X_1}} = 0.164433 + 0.661295 + 0.174272 = 1.000000$; etc.

It is not difficult to extend (38) by defining additional sequence family members. Note the turning points must match-up for adjacent potentials along the path. Also note the family number plus the sequence number (i.e.

$N = m + n$ for the potential matrix element $V_n^{(m)}$ of the last footnote) is the same for each potential belonging to a group with total $\Delta t = 1$, and this N increments by one as the particle moves from one potential group to the next.

V. CONCLUSION

The point of view supported in this paper is that the logistic map, and other discrete time-stepped dynamical models, may be regarded as continuously evolving Hamiltonian systems sampled at integer times. For this view to be valid, the continuous system must be allowed to undergo a series of switchbacks whereupon the potential affecting the dynamics changes when the evolving particle encounters a turning point. From a perspective of configuration space covering manifolds, in the case of simple one-dimensional motion, the particle moves from one sheet of a Riemann surface to another, to experience a different branch of the underlying analytic potential.

The methods of this paper may be used directly to determine such branches of the potential for the logistic map, for any value of s , as well as other one-dimensional maps. A more extensive study of other examples is underway [9]. While peculiar behavior is possible for exceptional maps (say, for special values[‡] of s), so far as we are aware, any such behavior can always be analyzed using the potential framework presented here.

In total, for all parameter values governing a particular map, the collection of potential sequence families constitute what we may call a “potential fractal” with self-similarities qualitatively evident in the various graphs, as visible in the above. Perhaps such potential fractals have a significant role to play in continuum physics. Applications might involve any of the usual systems exhibiting chaotic behavior [7], including accelerator beams [10], or perhaps cosmological models [11].

Acknowledgments

We thank David Fairlie, Xiang Jin, Luca Mezincescu, and especially Cosmas Zachos, for sharing their thoughts about functional evolution methods. One of us (TC) thanks the CERN Theoretical Physics Group for its gracious hospitality and generous support. The numerical calculations and graphics in this paper were made using Maple[®], Mathematica[®], and MuPAD[®]. This work was also supported by NSF Award 0855386.

-
- [1] T. Curtright and C. Zachos, *J. Phys. A: Math. Theor.* **42**, 485208 (2009), arXiv:0909.2424 [math-ph];
T. L. Curtright and C. K. Zachos, “Chaotic Maps, Hamiltonian Flows, and Holographic Methods” to appear in a well-known journal, *eventually*, arXiv:1002.0104 [nlin.CD].
 - [2] E. Schröder, *Math. Ann.* **3**, 296-322 (1871).
 - [3] R. M. May, *Nature* **261**, 459-467 (1976).
 - [4] P. Collet and J. P. Eckmann, *Iterated Maps On The Interval As Dynamical Systems*, Birkhäuser, Boston (1980).
 - [5] M. J. Feigenbaum, *Physica D* **7**, 16-39 (1983).
 - [6] L. Kadanoff, *Physics Today*, 46-53 (December 1983).
Also see http://en.wikipedia.org/wiki/Logistic_map .
 - [7] P. Cvitanović, et al., *Chaos: Classical and Quantum*, <http://chaosbook.org/> .
 - [8] For example, see <http://mathworld.wolfram.com/RadiusofConvergence.html> .
 - [9] T. Curtright and A. Veitia, in preparation.
 - [10] S. Y. Lee, *Accelerator Physics*, World Scientific (2004).
 - [11] G. C. Corrêa, T. J. Stuchi, and S. E. Jorás, *Phys. Rev.* **D81**, 083531 (2010), arXiv:1005.3273 [gr-qc].

[‡]A peculiar example is provided by $s = 1$. For this case the appropriate limit of (11) is not convergent but rather an asymptotic series. (See Appendix C.)

VI. APPENDIX A: FUNCTIONAL CONJUGATION

Functional conjugacy for the logistic map may be expressed in terms of a linear function. Namely,

$$g(sx(1-x)) = (2-s)g(x)(1-g(x)) , \quad (39)$$

where

$$g(z) = \frac{1}{2-s}(1-s+sz) , \quad g^{-1}(z) = \frac{1}{s}(s-1+(2-s)z) . \quad (40)$$

It is often useful to refer to these maps as $g(z) = g_s(z)$ and $g^{-1}(z) = g_{2-s}(z)$. Pursuing the conjugacy a bit farther, let $f_s(x) = sx(1-x)$, then the conjugacy equation for the map can be written in various ways:

$$g \circ f_s = f_{2-s} \circ g , \quad f_s \circ g^{-1} = g^{-1} \circ f_{2-s} , \quad (41)$$

$$g \circ f_s \circ g^{-1} = f_{2-s} , \quad g^{-1} \circ f_{2-s} \circ g = f_s . \quad (42)$$

Moreover, Schröder's equation is the functional composition

$$s \circ \Psi = \Psi \circ f_s , \quad (43)$$

where $s : x \rightarrow sx$ is the simple multiplicative map. Under functional conjugacy by g , the RHS of Schröder's equation becomes

$$g \circ \Psi \circ f_s \circ g^{-1} = g \circ \Psi \circ g^{-1} \circ f_{2-s} = \Psi_g \circ f_{2-s} \quad (44)$$

$$\Psi_g \equiv g \circ \Psi \circ g^{-1} \quad (45)$$

A. Alternate fixed point expansions

Consider again the logistic map, $x \mapsto sx(1-x)$. On the one hand, with a subscript to distinguish other constructions to follow, expansions about the trivial fixed point at $x = 0$ stem from:

$$s\Psi_0(x, s) = \Psi_0(sx(1-x), s) , \quad (46)$$

$$\Phi_0(sx, s) = s\Phi_0(x, s)(1-\Phi_0(x, s)) . \quad (47)$$

For the inverse Schröder functions, we consistently use the notation $\Phi = \Psi^{-1}$. On the other hand, expansions about the non-trivial fixed point at $x = 1 - 1/s$ stem from:

$$\lambda\Psi_*(z) = \Psi_*(\lambda z + (\lambda-2)z^2) , \quad (48)$$

$$\Phi_*(\lambda z) = \lambda\Phi_*(z) + (\lambda-2)\Phi_*^2(z) , \quad (49)$$

where

$$\lambda = 2-s , \quad s = 2-\lambda , \quad x = 1 - \frac{1}{s} + z , \quad z = x + \frac{1-s}{s} . \quad (50)$$

The two expansions produce *the same functions*, only slightly disguised. Here is the detailed relation between them, to be proved in the next subsection.

$$\Psi_*(z) = \frac{\lambda}{2-\lambda}\Psi_0\left(\frac{2-\lambda}{\lambda}z, \lambda\right) , \quad \text{i.e.} \quad \Psi_*\left(x + \frac{1-s}{s}\right) = \frac{2-s}{s}\Psi_0\left(\frac{s}{2-s}\left(x + \frac{1-s}{s}\right), 2-s\right) . \quad (51)$$

$$\Phi_*(z) = \frac{\lambda}{2-\lambda}\Phi_0\left(\frac{2-\lambda}{\lambda}z, \lambda\right) , \quad \text{i.e.} \quad \Phi_*\left(x + \frac{1-s}{s}\right) = \frac{2-s}{s}\Phi_0\left(\frac{s}{2-s}\left(x + \frac{1-s}{s}\right), 2-s\right) . \quad (52)$$

These relations are an extension of the previously known functional conjugacy that relates $s = 4$ and $s = -2$.

It is better notation to call the alternate series solutions $\Psi_*(x, s)$ and $\Phi_*(x, s)$, instead of $\Psi_*(z)$ and $\Phi_*(z)$. Then the “dual” parameter is

$$s_* = 2-s , \quad (53)$$

and the previous relations are more succinctly written as:

$$\Psi_*(x, s) = \frac{s_*}{s} \Psi_0\left(\frac{sx}{s_*}, s_*\right), \quad \Phi_*(x, s) = \frac{s_*}{s} \Phi_0\left(\frac{sx}{s_*}, s_*\right). \quad (54)$$

That is to say, the series solution of Schröder's equation for map parameter $2 - s$, about the trivial fixed point at $x = 0$, is conjugate to the series solution of Schröder's equation for map parameter s , about the nontrivial fixed point at $x_* = 1 - 1/s$. Now, as previously noted, functional conjugation by g gives (44) and (45). But then, $g \circ s \circ g^{-1}(u) = g(s - 1 + (2 - s)u) = \frac{(1-s)^2}{2-s} + su$, so

$$g \circ s \circ g^{-1} \circ \Psi_g(w, s) = \frac{(1-s)^2}{2-s} + s\Psi_g(w, s). \quad (55)$$

That is to say, the g -conjugated Schröder function obeys the inhomogeneous functional equation,

$$\frac{(1-s)^2}{2-s} + s\Psi_g(x, s) = \Psi_g((2-s)x(1-x), s), \quad (56)$$

whereas Ψ_* obeys a homogeneous equation, but with shifted position-dependent arguments.

$$(2-s)\Psi_*\left(x + \frac{1-s}{s}, s\right) = \Psi_*\left(sx(1-x) + \frac{1-s}{s}, s\right). \quad (57)$$

To summarize the relations between the various functions:

$$\Psi_0(x, s) = \frac{2-s}{s} \Psi_*\left(\frac{sx}{2-s}, 2-s\right), \quad (58a)$$

$$\Psi_*(x, s) = \frac{2-s}{s} \Psi_0\left(\frac{sx}{2-s}, 2-s\right), \quad (58b)$$

$$\Psi_g(x, s) = \frac{1-s}{2-s} + \Psi_*\left(x + \frac{s-1}{2-s}, 2-s\right) \quad (58c)$$

$$\Psi_*(x, s) = \frac{1-s}{s} + \Psi_g\left(x + \frac{s-1}{s}, 2-s\right) \quad (58d)$$

$$\Psi_g(x, s) = \frac{1-s}{2-s} + \frac{s}{2-s} \Psi_0\left(\frac{s-1+(2-s)x}{s}, s\right), \quad (58e)$$

$$\Psi_0(x, s) = \frac{s-1}{s} + \frac{2-s}{s} \Psi_g\left(\frac{1-s+sx}{2-s}, s\right), \quad (58f)$$

For the potential itself, functional conjugation leads to

$$V(x, s) = \left(\frac{2-s}{s}\right)^2 V\left(\frac{s}{2-s}\left(x - \left(1 - \frac{1}{s}\right)\right), 2-s\right), \quad (59)$$

$$U(x, s) = \left(\frac{(2-s)\ln(2-s)}{s\ln s}\right)^2 U\left(\frac{s}{2-s}\left(x - \left(1 - \frac{1}{s}\right)\right), 2-s\right). \quad (60)$$

Perhaps it is worthwhile to work out the various functions explicitly for the cases which can be solved in closed-form, with Ψ_0 and $\Phi_0 = \Psi_0^{-1}$ as given in (17). Consider the first and the last of these. The corresponding dual and conjugated functions are given by:

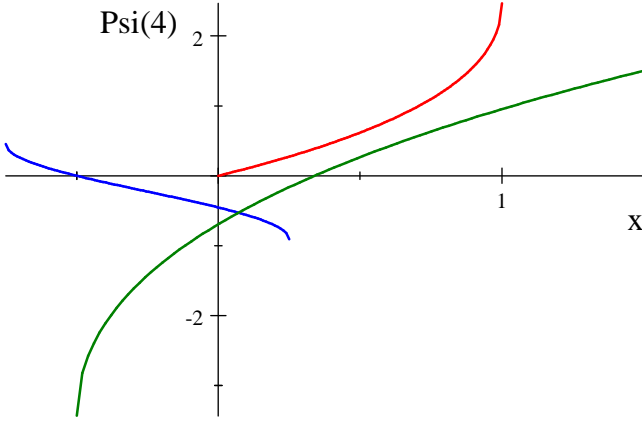
$$\Psi_*(x, 4) = -\frac{1}{2}\Psi_0(-2x, -2) = -\frac{\sqrt{3}}{12}\left(2\pi - 3\arccos\left(2x + \frac{1}{2}\right)\right), \quad (61a)$$

$$\Psi_*(x, -2) = -2\Psi_0\left(-\frac{1}{2}x, 4\right) = -2\left(\arcsin\sqrt{-\frac{1}{2}x}\right)^2, \quad (61b)$$

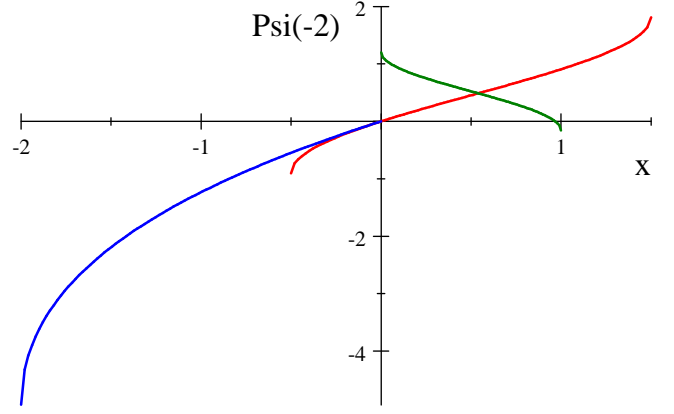
$$\Psi_g(x, 4) = \frac{3}{2} + \Psi_*\left(x - \frac{3}{2}, -2\right) = \frac{3}{2} - 2\left(\arcsin\sqrt{\frac{1}{2}\left(\frac{3}{2} - x\right)}\right)^2, \quad (61c)$$

$$\Psi_g(x, -2) = \frac{3}{4} + \Psi_*\left(x - \frac{3}{4}, 4\right) = \frac{3}{4} - \frac{\sqrt{3}}{12}(2\pi - 3\arccos(2x - 1)). \quad (61d)$$

We plot these, say for x such that the arguments of the inverse trigonometric functions are real, and the functions are principal-valued.



$\Psi_0(x, 4)$ red, $\Psi_*(x, 4)$ blue, and $\Psi_g(x, 4)$ green.



$\Psi_0(x, -2)$ red, $\Psi_*(x, -2)$ blue, and $\Psi_g(x, -2)$ green.

B. Alternate series solution theorem

Consider the Poincaré functional equation for the Schröder function inverse, rendered to facilitate expansion about the nontrivial fixed point “*” corresponding to $x_* = 1 - 1/s$,

$$\Phi_*((2-s)z, s) = (2-s)\Phi_*(z, s) - s\Phi_*^2(z, s) \quad \text{with} \quad \Phi_*(z, s) = z + O(z^2), \quad (62)$$

where

$$x = 1 - \frac{1}{s} + z, \quad z = x + \frac{1}{s} - 1. \quad (63)$$

Let

$$\Phi_*(z, s) = \frac{2-s}{s} \phi(z, s), \quad (64)$$

to change the functional equation to

$$\frac{2-s}{s} \phi((2-s)z, s) = \frac{(2-s)^2}{s} \phi(z, s) (1 - \phi(z, s)). \quad (65)$$

That is to say,

$$\phi((2-s)z, s) = (2-s)\phi(z, s) (1 - \phi(z, s)) \quad \text{with} \quad \phi(z, s) = \frac{sz}{2-s} + O(z^2). \quad (66)$$

Comparing this last relation to the original Poincaré functional equation tailored to yield the expansion about the trivial fixed point “0”,

$$\Phi_0(sx, s) = s\Phi_0(x, s) (1 - \Phi_0(x, s)) \quad \text{with} \quad \Phi_0(x, s) = x + O(x^2), \quad (67)$$

it follows that

$$\phi(z, s) = \Phi_0\left(\frac{sz}{2-s}, 2-s\right). \quad (68)$$

So then

$$\Phi_*(z, s) = \frac{2-s}{s} \Phi_0\left(\frac{sz}{2-s}, 2-s\right), \quad \Phi_0(z, s) = \frac{2-s}{s} \Phi_*\left(\frac{sz}{2-s}, 2-s\right), \quad (69)$$

and therefore the Schröder function, i.e. the inverse of the inverse function $\Psi = \Phi^{-1}$, is

$$\Psi_*(z, s) = \frac{2-s}{s} \Psi_0\left(\frac{sz}{2-s}, 2-s\right), \quad \Psi_0(z, s) = \frac{2-s}{s} \Psi_*\left(\frac{sz}{2-s}, 2-s\right). \quad (70)$$

Hence $\Phi_*(\Psi_*(z, s), s) = z = \Psi_*(\Phi_*(z, s), s)$. This proves the relationships between Φ_* , Ψ_* and Φ_0, Ψ_0 . ■

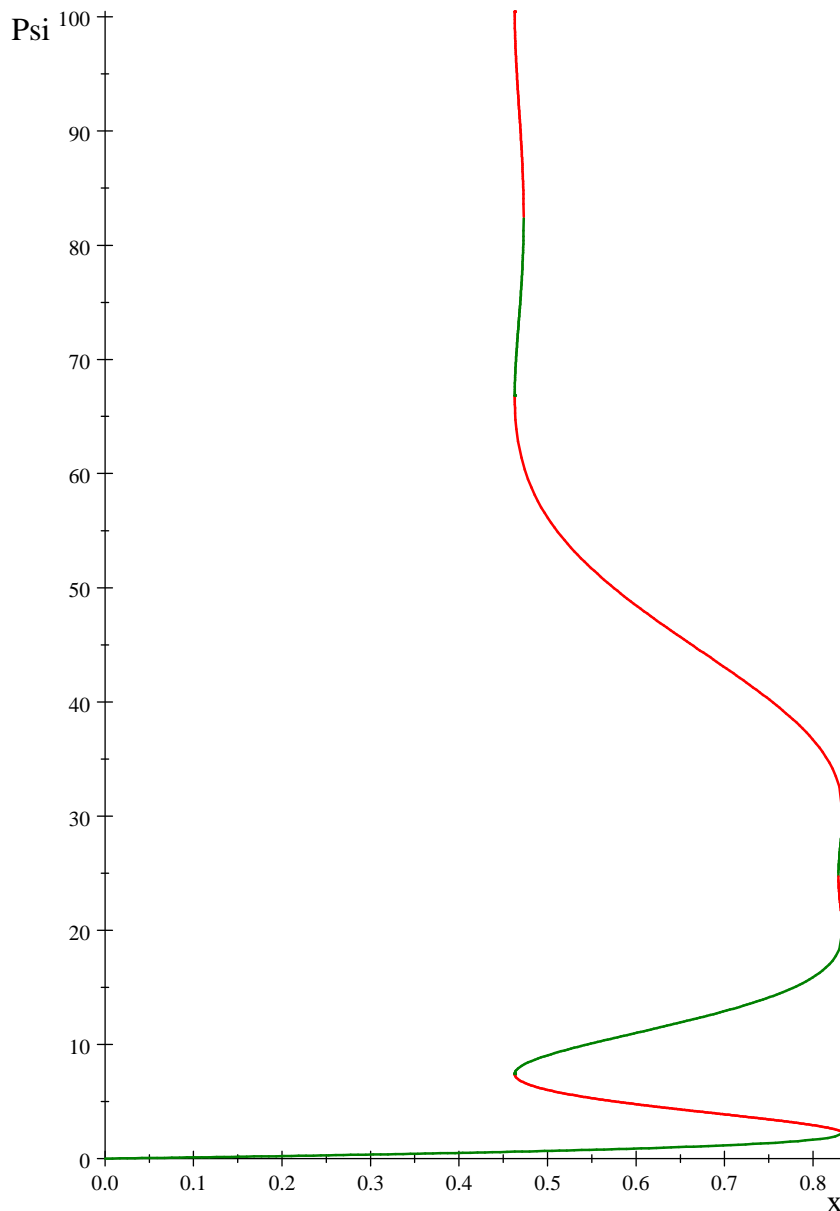
VII. APPENDIX B: CONSTRUCTING THE BRANCHES OF SCHRÖDER'S Ψ FUNCTION

We wish to imitate for $\Psi(x, s)$ what we did to find the branches of the potential in Section III of the text. We start with the functional equation, (8). Next we write $y = sx(1 - x)$, with solutions $x_{\pm} = \frac{1}{2} \left(1 \pm \sqrt{1 - 4y/s} \right)$. Now, we rename $y \rightarrow x$, so the functional relation becomes

$$\Psi_{\pm}(x, s) = s\Psi\left(\frac{1}{2}\left(1 \pm \sqrt{1 - 4x/s}\right), s\right). \quad (71)$$

One of these (Ψ_-) reproduces the original auxiliary function expanded about $x = 0$, only it does so more accurately for $x \rightarrow s/4$ as may be seen by numerical evaluation, while the other (Ψ_+) gives the auxiliary on another sheet of the function's Riemann surface. This is useful for determining the first switchback potential. The process may be repeated to get the other branches of the auxiliary as a sequence of functions, Ψ_n .

Here we are especially interested in $s = 10/3$, as we wish to confirm the order in which the switchback potentials are encountered by the evolving particle for this case. We find the following numerical results.



Eight branches of $\Psi(x, 10/3)$.

It follows that the order of the potentials is as given in the text: $V_0 \rightarrow V_1 \rightarrow V_2 \rightarrow W_1 \rightarrow W_2 \rightarrow V_3 \rightarrow X_1 \rightarrow X_2 \rightarrow \dots$.

As a practical matter, it is somewhat easier to compute the inverse function $\Phi \equiv \Psi^{-1}$ by combining series solution

methods with functional extensions. The functional equation for the inverse of Schröder's function is

$$\Phi(sx, s) = s\Phi(x, s) (1 - \Phi(x, s)) . \quad (72)$$

For $s < 1$ this quadratic equation may be solved for $\Phi(x)$ in terms of $\Phi(sx)$,

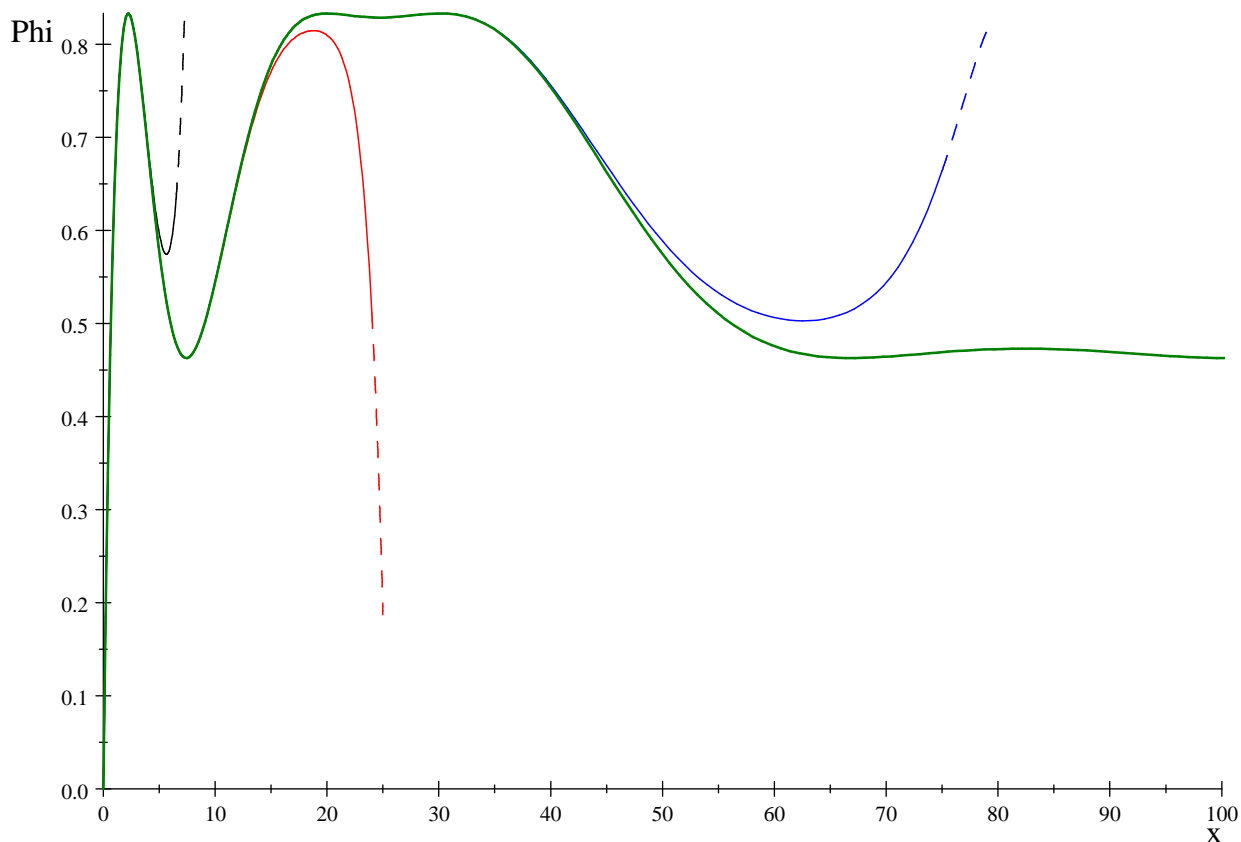
$$\Phi_{\pm}(x, s) = \frac{1}{2} \left(1 \pm \sqrt{1 - \frac{4}{s}\Phi(sx, s)} \right) , \quad (73)$$

and, upon iteration, all values of Φ may be obtained from those values given accurately by the series about $x = 0$. For $s > 1$, on the other hand, we first rescale x in (72) to write

$$\Phi(x, s) = s\Phi\left(\frac{x}{s}, s\right) \left(1 - \Phi\left(\frac{x}{s}, s\right)\right) , \quad (74)$$

and from this equation, upon iteration, all values of Φ may be obtained directly from those values given accurately by the series about $x = 0$.

As an example, consider again the case $s = 10/3$. We find:



Seventh order series approximation to $\Phi(x, 10/3)$, in black, compared to results from using this series in the 1st (red), 2nd (blue), and 3rd (green) iterates of the functional extension (74).

Flipping this graph about the SW-NE diagonal, we obtain a graph for the multi-valued $\Psi = \Phi^{-1}$. From the third iterate of (74) (as given in the graph by the green curve) the resulting curve for $\Psi(x, 10/3)$ agrees with the previous graph obtained by solving Schröder's equation through use of the series about $x = 0$, combined with functional methods.

VIII. APPENDIX C: THE $s = 1$ SERIES FOR THE POTENTIAL

For this case the appropriate limit of (11) gives

$$\begin{aligned} V(x, 1) &\equiv -\lim_{s \rightarrow 1} ((\ln^2 s) U(x, s)) \\ &= -x^4 - 2x^5 - 4x^6 - \frac{25}{3}x^7 - \frac{215}{12}x^8 - \frac{589}{15}x^9 - \frac{7813}{90}x^{10} - \frac{60481}{315}x^{11} - \frac{11821}{28}x^{12} + O(x^{13}) . \end{aligned} \quad (75)$$

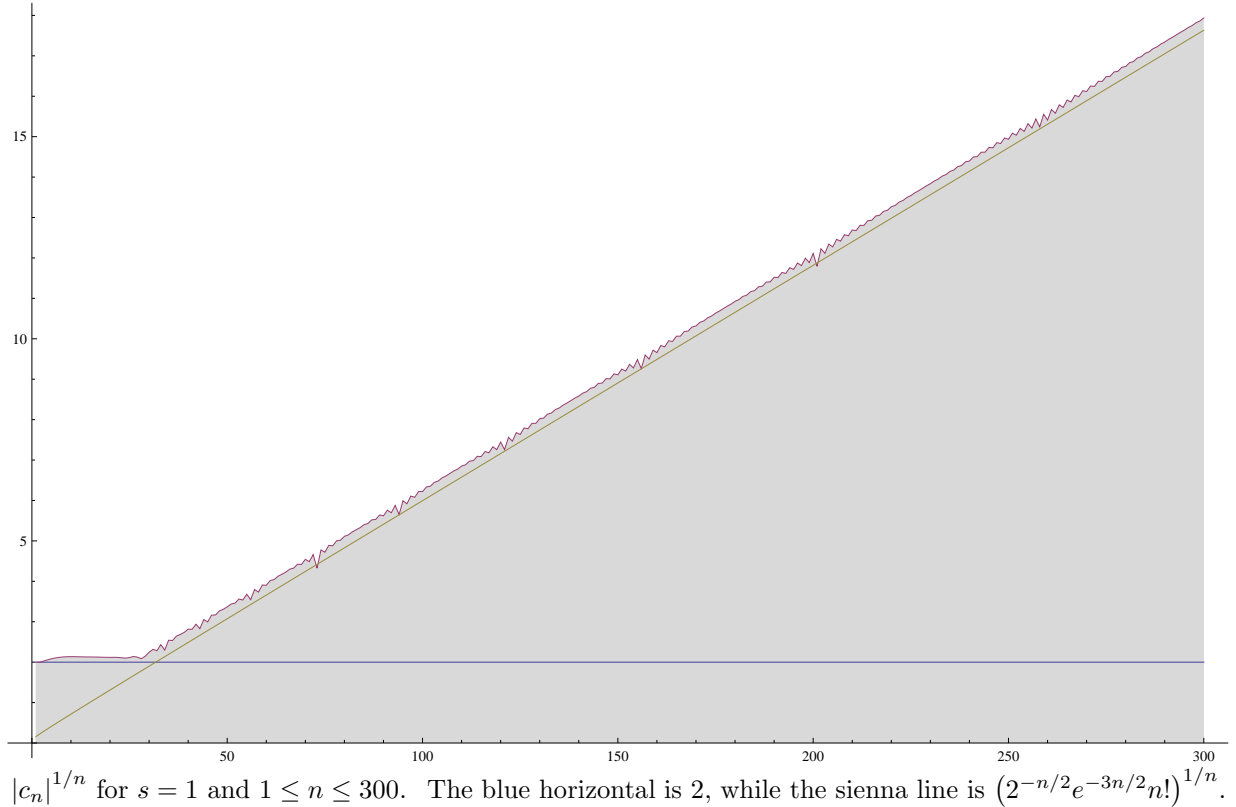
More systematically, let

$$V(x, 1) = -x^4 \left(1 + \sum_{n=1}^{\infty} c_n x^n \right), \quad c_1 = 2, \quad c_2 = 4, \quad c_3 = \frac{25}{3}, \dots, \quad (76)$$

and solve by iteration the functional equation that should be obeyed by $V(x, 1)$, namely,

$$V(x(1-x), 1) = (1-2x)^2 V(x, 1). \quad (77)$$

If the formal series (76) is constructed to $O(x^{25})$ or so, it appears to have a radius of convergence of $R \simeq 1/2$. But remarkably, this is seen to be illusory to higher orders. Different behavior sets in around $O(x^{30})$, where the successive $|c_n|^{1/n}$ used in the lim sup determination of R , (13), begin to grow linearly for $n > 30$, as shown here (purple curve, with wiggles).



$|c_n|^{1/n}$ for $s = 1$ and $1 \leq n \leq 300$. The blue horizontal is 2, while the sienna line is $(2^{-n/2} e^{-3n/2} n!)^{1/n}$.

That is to say, $|c_n| \sim L^n \exp(n \ln n)$ for large n , with $L \simeq \frac{16}{270} \simeq \frac{1}{\sqrt{2}e^{5/2}} = 5.80429 \times 10^{-2}$. This immediately brings to mind Stirling's formula, $n! \sim \sqrt{2\pi n} \left(\frac{n}{e}\right)^n$, and in fact, a comparison of c_n with $f_n \equiv 2^{-n/2} e^{-3n/2} n!$ is striking, as shown in the Figure. (The most important feature in the Figure is agreement between the averaged slopes. A better overall fit to the c_n , on average, is achieved by shifting the sienna line slightly to the left, for example by including an additional \sqrt{n} factor in f_n .)

All this is compelling evidence that (76) itself is *not* convergent, but rather an asymptotic series. Indeed, the f_n "fit" to c_n can be obtained from an asymptotic approximation of a simple integral:

$$\begin{aligned} I(x) &\equiv \int_0^{\infty} e^{-y} \frac{1}{1 - \frac{xy}{\sqrt{2}e^3}} dy = -\frac{\sqrt{2}}{x} \exp\left(\frac{3x - 2\sqrt{2}e^{\frac{3}{2}}}{2x}\right) \text{Ei}\left(1, -\frac{1}{x}\sqrt{2}e^{\frac{3}{2}}\right) \\ &= \int_0^{\infty} e^{-y} \sum_{n=0}^{\infty} x^n 2^{-n/2} e^{-3n/2} y^n dy \sim \sum_{n=0}^{\infty} f_n x^n. \end{aligned} \quad (78)$$

Taking the Cauchy principal value for $I(x)$ gives finite numerical results for all x . These results may be used to compute corrections to the polynomial approximation for $V(x, 1)$ as constructed from truncating the series (76). We leave further analysis of this interesting but peculiar case to the reader.